

This article was downloaded by: [McGill University Library]

On: 04 September 2014, At: 18:59

Publisher: Taylor & Francis

Informa Ltd Registered in England and Wales Registered Number: 1072954 Registered office: Mortimer House, 37-41 Mortimer Street, London W1T 3JH, UK



Philosophical Magazine

Publication details, including instructions for authors and subscription information:

<http://www.tandfonline.com/loi/tphm20>

On the effective permeability of a heterogeneous porous medium: the role of the geometric mean

P.A. Selvadurai^a & A.P.S. Selvadurai^b

^a Department of Civil and Environmental Engineering, University of California, Berkeley, CA, USA

^b Department of Civil Engineering and Applied Mechanics, McGill University, Montréal, QC, Canada

Published online: 13 May 2014.



CrossMark

[Click for updates](#)

To cite this article: P.A. Selvadurai & A.P.S. Selvadurai (2014) On the effective permeability of a heterogeneous porous medium: the role of the geometric mean, *Philosophical Magazine*, 94:20, 2318-2338, DOI: [10.1080/14786435.2014.913111](https://doi.org/10.1080/14786435.2014.913111)

To link to this article: <http://dx.doi.org/10.1080/14786435.2014.913111>

PLEASE SCROLL DOWN FOR ARTICLE

Taylor & Francis makes every effort to ensure the accuracy of all the information (the "Content") contained in the publications on our platform. However, Taylor & Francis, our agents, and our licensors make no representations or warranties whatsoever as to the accuracy, completeness, or suitability for any purpose of the Content. Any opinions and views expressed in this publication are the opinions and views of the authors, and are not the views of or endorsed by Taylor & Francis. The accuracy of the Content should not be relied upon and should be independently verified with primary sources of information. Taylor and Francis shall not be liable for any losses, actions, claims, proceedings, demands, costs, expenses, damages, and other liabilities whatsoever or howsoever caused arising directly or indirectly in connection with, in relation to or arising out of the use of the Content.

This article may be used for research, teaching, and private study purposes. Any substantial or systematic reproduction, redistribution, reselling, loan, sub-licensing, systematic supply, or distribution in any form to anyone is expressly forbidden. Terms &

Conditions of access and use can be found at <http://www.tandfonline.com/page/terms-and-conditions>

On the effective permeability of a heterogeneous porous medium: the role of the geometric mean

P.A. Selvadurai^{a*} and A.P.S. Selvadurai^b

^aDepartment of Civil and Environmental Engineering, University of California, Berkeley, CA, USA; ^bDepartment of Civil Engineering and Applied Mechanics, McGill University, Montréal, QC, Canada

(Received 16 October 2013; accepted 4 April 2014)

This paper uses experimental data derived from surface permeability tests conducted on a bench-scale 508 mm cuboidal sample of Indiana Limestone. These results are used in combination with computational modelling to test the hypothesis that the geometric mean is a good proxy to represent permeability when the spatial distribution of the permeability for the heterogeneous rock, with no evidence of hydraulic anisotropy or fractures, is log-normal. The predictive capabilities of the geometric mean as a measure of the effective permeability are further assessed by examining specific examples where three-dimensional flows are initiated in the heterogeneous domain and where the equivalent homogeneous problem gives rise to purely circular flows that have exact solutions. The approach is also applied to examine a hypothetical hydraulic pulse test that is conducted on a cuboidal region with sealed lateral boundaries, consisting of the experimentally measured heterogeneous distribution of permeability and an equivalent homogeneous region where the permeability corresponds to the geometric mean.

Keywords: permeability heterogeneity; effective permeability; surface permeability tests; computational developments; geometric mean; hydraulic pulse tests

1. Introduction

Naturally occurring intact geologic media have heterogeneous material characteristics that are scale-dependent. In particular, the fluid transmissivity properties of such porous media are sensitive to inhomogeneities that can exist at any scale. These can range from inhomogeneities at the micro-scale resulting from defects such as micro-cracks and porous inclusions present in the scale of a laboratory test specimen, to inhomogeneities at the regional scale resulting from, for example, faults, fractures, stratifications or dissolution channels. To accurately characterize, the permeability of heterogeneous porous media is important in many areas of modern environmental geosciences and environmental geomechanics; key applications focus on earth-borne migration of contaminants [1–3], deep geologic disposal of hazardous substances such as heat-emitting nuclear waste [4–7], earthquake hazards along fault zones [8–10], geothermal energy extraction [11,12] and, more recently, the geologic disposal of carbon dioxide as

*Corresponding author. Email: patrick.selvadurai@mcgill.ca

a means of mitigating climate change through reduction of greenhouse gases in the atmosphere [13–16]. In all these endeavours, the permeability of the geologic medium is a parameter of critical interest and governs much of the dominant thermo-hydro-mechanical-chemical processes. Various approaches have been proposed in the literature for characterizing permeability in heterogeneous formations and references to these can be found in the texts and articles [17–26]. While the complete non-deterministic characterization of permeability heterogeneity is certainly possible (see. e.g. [20,27–31]), the use of such approaches in computational simulations of large-scale porous media flow problems can be complex and computing intensive if both heterogeneity and anisotropy are simultaneously introduced to characterize variability. The more pragmatic approaches to characterization of permeability of heterogeneous porous geomaterials retain the overall structure of a porous medium that is modelled either as homogeneous and isotropic or homogeneous and anisotropic, and captures the overall influences of heterogeneity by representing the permeability through *effective* estimates. The influences of heterogeneities are thus averaged out over a Representative Volume Element (RVE). Even with such simplifications, the separation of the influences of heterogeneity and anisotropy can be scale-dependent. It is well known that a stratified porous medium that is isotropic and heterogeneous at the scale of the thickness of the strata unit can be viewed as a porous medium that is homogeneous and anisotropic at scales with dimensions significantly larger than this local length scale; i.e. the RVE selected can ultimately influence the model selected to simulate flow through the porous medium.

The objective of this paper is to employ results of recent experimental research (see [24]), conducted on a cuboidal specimen of Indiana Limestone measuring 508 mm, to further investigate computational approaches for establishing effective permeability of a heterogeneous porous medium. It should be noted that, although widely used, Indiana Limestone is not a standard geologic material and, within the same horizon, there can be variability. An important and informative study [32] documents the petrographic properties, and indicates that the rocks generally consist of calcite (99%), with the remainder being quartz. In this study [32], the calcite cemented grainstone is made up of fossil fragments and oolites [33]. Similar observations were made for the Indiana Limestone used in the research investigations conducted by Glowacki [34], Mattar [35] and Selvadurai [36]. The physical (density, porosity) and mechanical properties (Young's modulus, Poisson's ratio) of the Indiana Limestone used in the present experiments compare favourably with values for the buff-coloured Indiana Limestone reported in the literature. Since the stress states encountered in the permeability experiments are nominal, we can expect the fabric to remain sensibly constant throughout the research investigation. The chemical compatibility of the water used to perform the permeability tests can be an issue if there is either dissolution or dissolution and precipitation in the porous fabric. The study by Churcher et al. [32] indicated trace amounts of illite and kaolinite; these fines were less than 2 μm and could be mobilized during permeability tests. However, they concluded that the minute amounts of clay minerals were unlikely to cause plugging problems during permeability testing. The determination of the micro-structural characteristics is certainly a non-routine task and requires access to sophisticated experimental facilities (see e.g. [37]), which were unavailable to the research group.

The near surface permeability of the cuboidal region was examined using novel experimental techniques involving an annular permeameter. The experimental results

were used to construct a spatial distribution of hydraulic heterogeneity within the cuboidal specimen. Upon verification of the absence of dominant pathways for fluid flow within the cuboidal region, estimates were obtained for the *Effective Permeability* of the cuboid using the mathematical relationships proposed by [38–43], among others.

This paper considers an idealized heterogeneous porous medium composed of sub-cuboidal units of homogeneous permeability. The permeabilities within the group of sub-cuboidal regions conform to a *log-normal* distribution similar to the experimental work presented in the paper. Effective permeability for the region is established using the *geometric mean concept*, and the accuracy of this proxy is verified via computational modelling of flow within arbitrarily oriented cuboidal, annular and toroidal sectors, which are sub-regions of the larger heterogeneous cuboidal domain, that are subjected to appropriate boundary potentials. Finally, the predictive capabilities of the geometric mean-based measure of the effective permeability is further tested in situations where transient fluid flow is induced in a hypothetical geomaterial with a log-normal, heterogeneous permeability distribution, similar to conditions that can be present in a conventional one-dimensional axial flow hydraulic pulse test.

2. Governing equations

For completeness, we briefly outline the problem of transient flow in a porous medium considering the influences of heterogeneity and illustrate the reduction to the classical equations governing steady state and transient flows when the local homogeneity assumption is invoked. In the absence of mass generation or mass loss, it can be shown that the equation of mass conservation is given by

$$\frac{\partial}{\partial t} \{ \rho n^*(\mathbf{x}) \} + \nabla \cdot \{ \rho \mathbf{v}_v(\mathbf{x}) n^*(\mathbf{x}) \} = 0 \quad (1)$$

where ρ is the mass density of the fluid, $n^*(\mathbf{x})$ is the position dependent porosity and $\mathbf{v}_v(\mathbf{x})$ is the velocity vector in the pore space. The pore velocity is related to the spatially averaged velocity through the relationship $\mathbf{v}(\mathbf{x}) = n^*(\mathbf{x}) \mathbf{v}_v(\mathbf{x})$. Considering the compressibility of the pore fluid and the porous skeleton, the result (1) can be written as

$$\left(n^*(\mathbf{x}) + \frac{C_{sk}(\mathbf{x})}{C_w} \right) \frac{\partial \rho}{\partial t} + \nabla \cdot \{ \rho \mathbf{v}(\mathbf{x}) \} = 0 \quad (2)$$

where $C_{sk}(\mathbf{x})$ is the position-dependent compressibility of the porous skeleton and C_w is the compressibility of the pore fluid. For an inhomogeneous but locally isotropic porous medium, Darcy's law governing fluid flow through the porous medium can be expressed in terms of the spatially averaged measure of the flow velocity as follows:

$$\mathbf{v}(\mathbf{x}) = - \left(\frac{K(\mathbf{x}) \gamma_w}{\mu} \right) \nabla \Phi \quad (3)$$

where $K(\mathbf{x})$ is the position-dependent isotropic permeability, γ_w is the unit weight of water, μ is the dynamic viscosity, Φ is the reduced Bernoulli potential, which consists of the pressure potential ($\Phi_p = p(\mathbf{x}, t) / \gamma_w$ where $p(\mathbf{x}, t)$ is the fluid pressure) and datum

potential (Φ_d) and ∇ is the gradient operator. We assume that the fluid density varies with the fluid pressure as follows:

$$\rho = \rho_0 \exp[C_w(p - p_0)] \tag{4}$$

where p_0 is a reference pressure, ρ_0 is the reference density of the fluid and when the fluid is incompressible, $C_w = 0$ and $\rho = \rho_0$. The above results can be used to express the mass conservation equation in the form

$$\left(\frac{K(\mathbf{x})}{\mu[n^*(\mathbf{x})C_w + C_{sk}(\mathbf{x})]} \right) \left\{ \nabla^2 \Phi + \nabla \Phi \left(\frac{\nabla K(\mathbf{x})}{K(\mathbf{x})} \right) \right\} = \frac{\partial \Phi}{\partial t} \tag{5}$$

where ∇^2 is Laplace's operator. The local homogeneity implies that in a non-dimensional version of (5), the term $\nabla \Phi (\nabla K(\mathbf{x})/K(\mathbf{x}))$ can be neglected in relation to the term involving the second-order operator and, as a consequence, (5) can be reduced to the form

$$\left(\frac{K(\mathbf{x})}{\mu[n^*(\mathbf{x})C_w + C_{sk}(\mathbf{x})]} \right) \nabla^2 \Phi = \frac{\partial \Phi}{\partial t} \tag{6}$$

The result (6) is the conventional piezo-conduction or elastic drive equation associated with transient hydraulic processes in a heterogeneous porous medium. In the limit when the porous medium is non-deformable (i.e. $C_{sk}(\mathbf{x}) \rightarrow 0$), the fluid is incompressible (i.e. $C_w \rightarrow 0$) and $\nabla \Phi (\nabla K(\mathbf{x})/K(\mathbf{x}))$ can be neglected, so that (6) reduces to Laplace's equation

$$\nabla^2 \Phi(\mathbf{x}) = 0 \tag{7}$$

3. Analysis of steady flow

The experimental configuration used to estimate the surface permeability of the cuboidal block of Indiana Limestone involves the application of steady flow to the central part of an annular sealed region (inner radius a and outer radius b) of a permeameter that can be placed at any location of a plane face of the cuboid, as shown in Figure 1(a). The dimensions of the permeameter in terms of the ratio b/a are such that the potential problem can be formulated as a three-part mixed boundary value problem in potential theory for a halfspace region governed by (7). When the annular permeameter is located centrally and on a plane face of the block, the boundary conditions take the form

$$\begin{aligned} \Phi(r, 0) &= \Phi_0, & r \in (0, a) \\ \left(\frac{\partial \Phi}{\partial z} \right)_{z=0} &= 0, & r \in (a, b) \\ \Phi(r, 0) &= 0, & r \in (a, \infty) \end{aligned} \tag{8}$$

It should be noted that the reduced Bernoulli potential $\Phi(\mathbf{x})$ includes the datum potential and the pressure potential. The pressure potential is measured with reference to the atmospheric pressure. The surface permeability testing technique proposed by Selvadurai and Selvadurai [24] involves a movable annular sealing patch that is placed on the plane

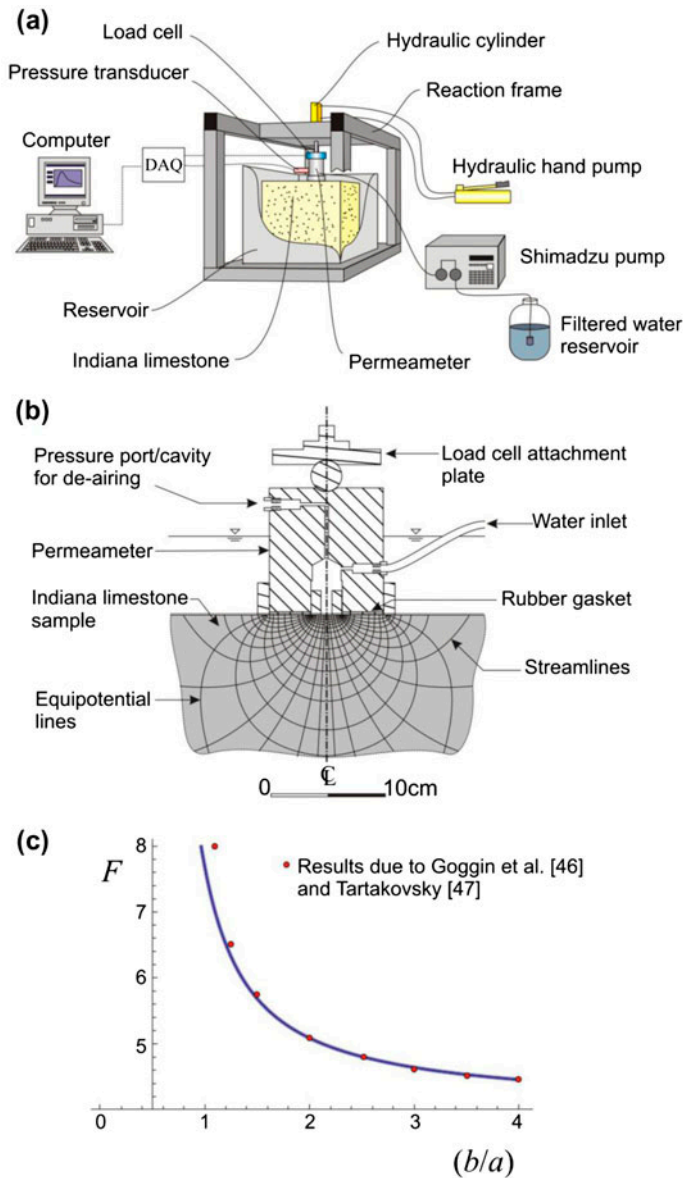


Figure 1. (colour online) Experimental facilities used by Selvadurai and Selvadurai [24] to determine surface permeability on a cuboidal block of Indiana Limestone (508 mm). (a) The general arrangement of the laboratory-scale surface permeability test and details of the test setup. (b) A cross-sectional view of the permeameter including a flow pattern in the vicinity of the permeameter. (c) Influence of the geometry of the annular sealing patch on the intake shape factor.

surface of a saturated cuboidal block of Indiana Limestone (Figure 1(b)). The uniform potential applied to the central aperture induces a constant flow rate Q . The three-part boundary value problem in potential theory defined by (8) has no exact analytical

solution. A procedure for obtaining an approximate solution was presented by Selvadurai and Singh [44,45]. The near surface permeability at each location is obtained from the result

$$K = \frac{Q\mu}{4a\Phi_0\gamma_w F(c)} \quad (9)$$

where

$$F(c) = 1 + \left(\frac{4}{\pi^2}\right)c + \left(\frac{16}{\pi^4}\right)c^2 + \left(\frac{64}{\pi^6} + \frac{8}{9\pi^2}\right)c^3 + \left(\frac{64}{9\pi^4} + \frac{256}{\pi^8}\right)c^4 + \left(\frac{92}{225\pi^4} + \frac{384}{9\pi^6} + \frac{1024}{\pi^{10}}\right)c^5 + O(c^6) \quad (10)$$

and $c = (a/b) \ll 1$ is the aperture ratio. Selvadurai and Selvadurai [24] showed that this analytical result, albeit approximate, is in excellent agreement with results obtained by Goggin et al. [46] and Tartakovsky et al. [47] using alternative numerical solutions of the system of triple integral equations (Figure 1(c)). Also it is noted that when $c \rightarrow 0$ (i.e. the outer boundary of the sealing annulus is remotely located), the three-part boundary value problem (8) reduces to a classical two-part mixed boundary value problem in potential theory for a halfspace and (8) reduces to $K = Q\mu/4a \Phi_0\gamma_w$, which is a concise result that can be used to estimate the local permeability of the tested region. It has also been shown [24] that the estimation of local permeability using the annular sealing patch permeameter is relatively uninfluenced by the permeability heterogeneity of the regions surrounding the permeameter and that the result for the case $c \rightarrow 0$ can be used quite effectively to estimate the local permeability of the porous medium. The validity of the assumption can be proven by considering a hypothetical surface permeability test conducted on a single cuboidal sub-region where the exterior permeabilities of the regions adjacent to the plane faces are assigned extreme values (i.e. either *infinite* permeability or *zero* permeability). If the permeability of the cuboidal sub-region is assumed to be homogeneous, and if the permeabilities are determined by the application of the two extreme classes of boundary conditions to the sides of the cube (excluding the side containing the permeameter), then the difference in the estimated values for the permeabilities is less than 5.43%, which is considered sufficient for purposes of permeability estimation. It must be remarked that for this hypothesis to be applicable, the near surface permeability in the vicinity of the open tip of the permeameter should be relatively uniform. The local permeability was determined at nine locations on each of the six surfaces of the cuboidal block of Indiana Limestone. The nine locations correspond to the interior nine points of the grids as shown in Figure 2. The 54 local surface permeability measurements were then used to estimate, via a kriging procedure, the spatial distribution on the set of 64 cuboidal sub-regions: the surface values thus obtained on three faces are shown in Figure 2(a). The log-normal permeability distribution of the 64 sub-regions is shown in Figure 2(b). The selection of the 64 cuboidal regions provides estimates that can be used for convenient comparison with results of computational modelling.

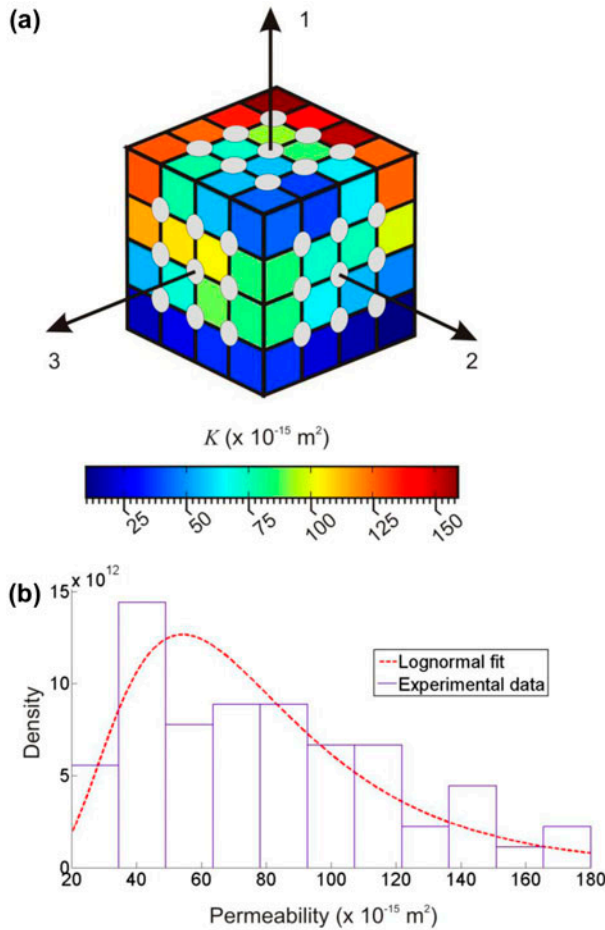


Figure 2. (colour online) Spatial distribution of permeability; results from Selvadurai and Selvadurai [24].

4. Computational modelling of steady flow

The generated spatial distribution of the point-wise isotropic permeability in the 64 sub-cubes provides a basis for estimating the effective permeability of the cuboidal block of Indiana Limestone. We first establish the conformity of the data-set to a log-normal statistical distribution. Figure 2(b) shows the comparison between the experimental data for the permeability values and the ideal log-normal distribution. The set of measured and kriged values of permeability also satisfies the *Kolmogorov-Smirnoff Test* [48] and establishes the applicability of the log-normal distribution with a 95% confidence level. The estimates for the effective permeability of the cuboidal region can be determined through computational modelling, where the entire cuboidal region is discretized into 136,247 tetrahedral finite elements. The computational modelling was performed using the multi-physics code COMSOL™. The concept of a homogeneous estimate for the effective permeability becomes meaningful only if there are no dominant or preferred

paths of fluid flow (e.g. fractures, solution channels, damaged regions, etc.) that can unduly influence the estimation of effective permeability. It must be emphasized that the heterogeneity should be uniformly distributed according to a log-normal distribution and this is well known in hydrogeological practice [49]. This requirement can be assessed by performing computational simulations where one-dimensional Darcy flows are initiated through the cuboid with the heterogeneous distribution of permeability in the sub-cube regions. The one-dimensional permeability in the three orthogonal directions is estimated at

$$K_1 = 78.44 \times 10^{-15} \text{ m}^2; \quad K_2 = 78.98 \times 10^{-15} \text{ m}^2; \quad K_3 = 64.76 \times 10^{-15} \text{ m}^2 \quad (11)$$

where the subscripts 1, 2 and 3 do not relate to the principal directions. The computations indicate a nominal measure of directional dependence, which is within a range that can justify the applicability of the effective permeability concept (i.e. a permeability ratio 1.000: 1.007: 0.826). An *order of magnitude* mismatch in the permeability values in any set of (orthogonal) directions could be regarded as a limit on the directional dependence that would permit the applicability of the procedure advocated in the present paper. The proposed geometric mean concept can be stated as follows: *Consider a heterogeneous porous medium with a spatial distribution of point-wise isotropic permeability that corresponds to a log-normal distribution. If hydraulically constrained one-dimensional permeability through this region measured in n directions is denoted by K_i ($i = 1, 2, \dots, n$), then the effective permeability of the porous medium of the region is given by the geometric mean*

$$K_{eff}^{SS} = \sqrt[n]{K_1 K_2 K_3 \dots K_n} \quad (12)$$

provided $n \geq 3$.

Again, it must be emphasized that the geometric mean-based representation of effective permeability of the porous medium with hydraulic heterogeneity in the domain *does not extend* to fractured media or media with dominant permeability stratification. In such instances, the representation of the effective permeability in terms of the geometric mean has limitations. As an example, consider a geologic medium that is nearly impermeable but contains a set of parallel fractures, which gives rise to a fracture permeability K_t in the plane of the fractures. Since the geological material is nearly impervious, the permeability perpendicular to the fractures will be zero; i.e. $K_n = 0$. If the geometric mean concept is applied to the fractured medium, the effective permeability estimated using (12) will be zero, whereas the fractured medium is permeable. Also, as has been shown by [26], if the permeameter is in contact with a *hydraulically transversely isotropic medium* with permeabilities K_t and K_n , where the plane of transverse isotropy is inclined at an angle α to the circular entry point, the result equivalent to (9) with $c \rightarrow 0$, takes the form

$$Q = \frac{2\pi a \gamma_w}{\mu K(\rho)} \left(\cos^2 \alpha + \frac{K_t}{K_n} \sin^2 \alpha \right) \sqrt{K_t K_n} \Phi_0 \quad (13)$$

where $K(\rho)$ is the complete elliptic integral and

$$\rho = \sqrt{\frac{(K_t - K_n) \sin^2 \alpha}{K_t \sin^2 \alpha + K_t \cos^2 \alpha}} \quad (14)$$

Clearly, a single permeability test with a circular entry point is *insufficient* to determine both K_t and K_n . If the orientation of the stratification is parallel to the plane of the permeameter, $\alpha = 0$ (i.e. $\rho = 0$, $K(0) = \pi/2$) and (13) reduces to

$$Q = \frac{4a\gamma_w \sqrt{K_t K_n}}{\mu} \quad (15)$$

Here, the permeability measured in the test would be the geometric mean of the stratified medium and if $K_n \rightarrow 0$ (i.e. a condition similar to a fractured medium indicated previously), $K_{eff}^{SS} \rightarrow 0$, whereas the medium is permeable. The geometric mean concept therefore should only be applied after giving due consideration to the nature of the heterogeneity (dominant stratifications, fractures, wormholes, etc.).

For a heterogeneous medium without defects, we can use the relationship (12) and the data-set (11) to obtain

$$K_{eff}^{SS} = 73.75 \times 10^{-15} \text{ m}^2 \quad (16)$$

The estimate (16) compares favourably with results obtained using several mathematical relationships available in the literature for estimating the effective permeability of a heterogeneous porous medium and is within the Wiener [38] bounds for the permeability (i.e. the *arithmetic* and *harmonic* means).

The computational investigations are then extended to create a synthetic porous medium where 1000 elements are randomly assigned permeability values that corresponded to a log-normal distribution of permeability (Figure 3) and where the permeabilities of the individual 1000 isotropic sub-elements are in the range $K \in (18.5 \times 10^{-15} \text{ m}^2, 318 \times 10^{-15} \text{ m}^2)$. The corresponding data-set conforms to a log-normal distribution that satisfies the Kolmogorov–Smirnov test with a log-mean of -30.275 and variance of 0.2559 , which conforms to the actual experimental results discussed previously. The effective permeability of the 1000 element synthetic cuboidal domain can be estimated by performing computational simulations of one-dimensional flow along three orthogonal directions coincident with the edges of the cuboidal domain. The finite element simulations were conducted using COMSOL™ and employed 51,468 tetrahedral elements, which is considered sufficient to provide accurate results for calculating the effective permeability. The Wiener [38] bound estimates for the effective permeability for the cuboidal region shown in Figure 3 gave the following:

$$K_{LB}^W \leq K_{eff} \leq K_{UB}^W \quad (17)$$

where $K_{LB}^W \approx 63.39 \times 10^{-15} \text{ m}^2$ and $K_{UB}^W \approx 79.79 \times 10^{-15} \text{ m}^2$. There is evidence of heterogeneity in the permeability since the upper and lower Wiener bounds do not coincide but the heterogeneity in the synthetic sample does not contribute to any dominant

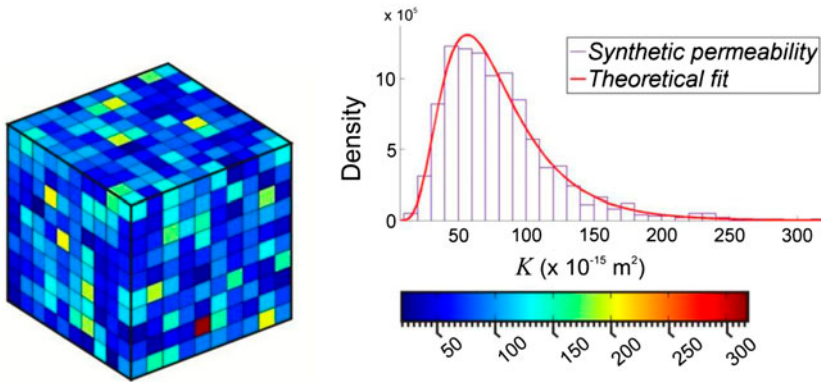


Figure 3. (colour online) Cuboidal domain with hydraulic heterogeneity.

planes of stratification that would lead to effective permeability mismatch of several orders of magnitude. The geometric mean concept for the estimation of the effective permeability (12), based on impervious boundary rectilinear one-dimensional permeability estimates obtained along three orthogonal directions, gives

$$\left[K_{eff}^{SS} \right]_{\text{Rectilinear}} \approx 73.96 \times 10^{-15} \text{ m}^2 \tag{18}$$

We next consider the effective permeability of an oriented cuboidal sub-region that is contained within the larger cuboidal domain, as shown in Figure 4. Since the heterogeneity has no directional dependence, the orientation of the cuboidal sub-region should not influence the estimation of the effective permeability based on the geometric mean. The choice of the orientation of the sub-region used to estimate the effective permeability is therefore entirely arbitrary. The volume of the sub-region in relation to the volume of the larger cuboidal domain is 0.2441. The computationally derived geometric mean-based effective permeability for the sub-region, with orthonormal basis $\{\hat{e}^i\}_{i=1}^3$, is

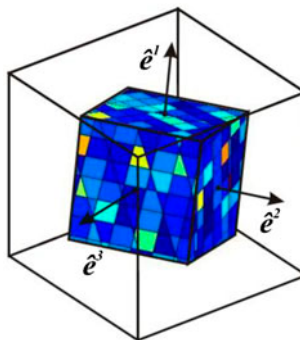


Figure 4. (colour online) An oriented sub-cuboidal region within the cuboidal domain shown in Figure 3.

$$[K_{eff}^{SS}]_{Oriented} \approx 74.18 \times 10^{-15} \text{ m}^2 \quad (19)$$

which is consistent with the estimates given by (16) and (18) for the larger cuboidal region.

5. Computational modelling of circular flow

The estimations of effective permeability using the geometric mean concept presented in the previous section were based on values derived by inducing impervious boundary, rectilinear Darcy flow within cuboidal regions defined by two different orthonormal basis. It is natural to enquire whether the conjecture for the estimation of the effective permeability based on this assumption extends to the prediction of flow rates encountered with other types of flow patterns within the cuboidal domain. There are many such flow patterns that can be considered for assessing the accuracy of the conjecture; in this section, we shall consider circular flow within *annular* and *toroidal* regions. The type of problem examined in these flow situations can be applied to examine subsurface flows, particularly in the vicinity of water retaining structures such as dams, where near circular flows can develop due to head differences [50–52].

We consider the problem of flow within an annular sector located inside the cuboidal domain as shown in Figure 5. Constant potential boundary conditions are prescribed over two of the plane surfaces and null Neumann boundary conditions are prescribed over the cylindrical surfaces and the remaining planes. For an annular cylindrical sector region of homogeneous permeability K , inner radius a and outer radius b , where the plane ends are subjected to potential difference Φ_0 , the permeability is related to the flow rate Q through the relationship

$$K = \frac{\pi Q \eta}{2 \gamma_w b \Phi_0 \log_e(b/a)} \quad (20)$$

The orientation of the annular sectors can be arranged in such a way that the effective permeability can be calculated using the separate annular sectors shown in Figure 6.

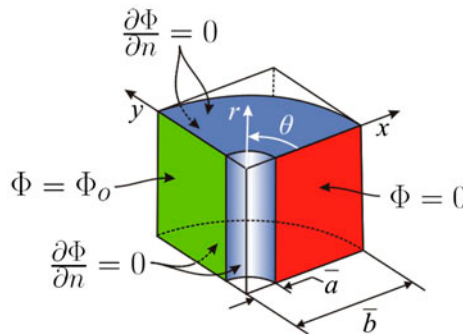


Figure 5. (colour online) Circular flow within an annular sector inside the cuboidal domain.

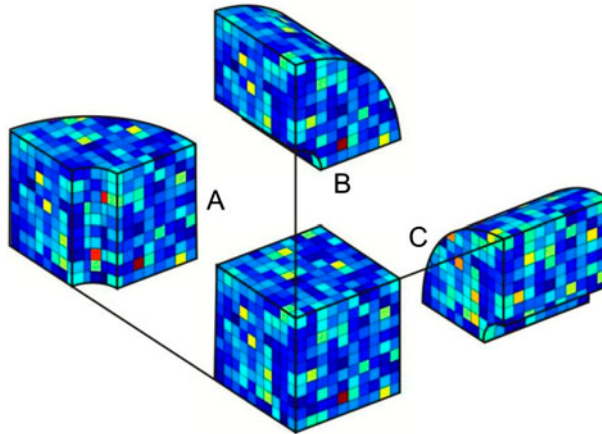


Figure 6. (colour online) Annular sectors selected for examining circular flows.

We note that the ratio of the volume of an annular sector to the volume of the cuboidal domain is 0.7378. The maximum and minimum Wiener [38] bounds derived from *all three annular sectors* give the following estimates for the effective permeability:

$$(63.213)10^{-15} \text{ m}^2 \leq K_{eff} \leq (80.371)10^{-15} \text{ m}^2 \tag{21}$$

Separate estimates for the permeability of an annular region based on the circular flow can be calculated using the result (20), which is used in conjunction with (12) to determine the effective permeability, where the permeabilities K_i are based on the values derived from the three separate *circular flow* problems associated with sub-domains in the cuboidal region. The geometric mean for the effective permeability gives

$$\left[K_{eff}^{SS} \right]_{Annular} \approx 74.00 \times 10^{-15} \text{ m}^2 \tag{22}$$

This result is remarkably close to the values obtained from the geometric mean-based estimates for the effective permeability derived from the rectilinear Darcy flows associated with the full cuboid given by (18) and the oriented interior sub-cube given by (19).

As a further illustration of the applicability of the geometric mean-based estimate for the effective permeability, we consider the problem of flow within the segment of a porous toroid as shown in Figure 7. The ratio of the volume of the segment of toroid with respect to the volume of the larger cuboidal domain is 0.395. In this case, the plane faces of the sector of the toroid are subjected to constant potentials and the curved boundary of the segment of the torus is subjected to null Neumann conditions. To the authors' knowledge, there is no analytical result for the problem of flow within a heterogeneous or homogeneous porous toroidal sector. The analysis of the problem is therefore approached in the following manner: In the first study, the fluid flow rate $(Q)_{K-distributed}$ through the toroidal sector is calculated using the *exact distribution of hydraulic heterogeneity* for the large cuboidal region shown in Figure 8. In the second computation, the flow rate $(Q)_{K-Effective}$ is calculated using a *geometric mean-based*

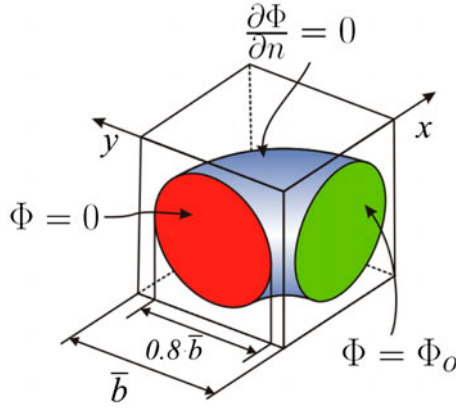


Figure 7. (colour online) Circular flow within a toroidal sector inside the cuboidal domain.

effective permeability of the sector, which is obtained from an average of the effective permeabilities determined from the oriented sub-cube given by (19) and the annular sector value given by (22). Considering one orientation of the toroidal region, we have

$$\frac{(Q)_{K\text{-Effective}}}{(Q)_{K\text{-Distributed}}} \approx 74.00 \times 10^{-15} \text{ m}^2 \tag{23}$$

Considering all three orientations of the toroidal regions as shown in Figure 8, the range of values for (23) is obtained as follows:

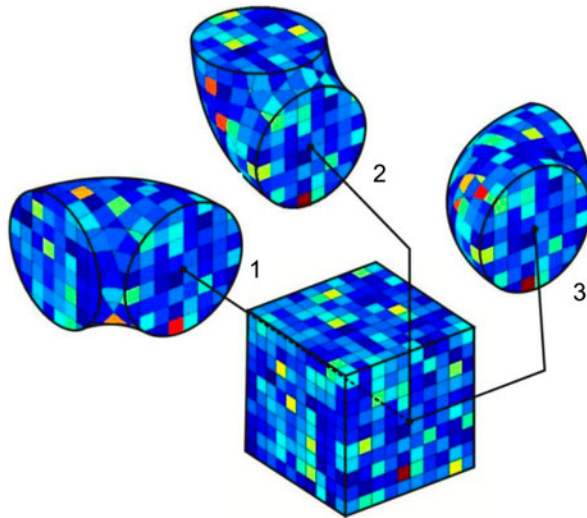


Figure 8. (colour online) Circular flow within toroidal sectors.

$$\frac{(Q)_{K\text{-Effective}}}{(Q)_{K\text{-Distributed}}} \in (0.963, 0.987) \tag{24}$$

6. Transient flow in an inhomogeneous porous medium

We now extend the basic concepts associated with the representation of hydraulic heterogeneity through the geometric mean to examine the spatially one-dimensional hydraulic pulse tests conducted under hydraulically boundary constrained one-dimensional conditions. The consideration of transient effects also introduces other material parameters in the description of the transient hydraulic pulse tests, and these include the permeability $K(\mathbf{x})$, the elastic modulus $E(\mathbf{x})$, Poisson’s ratio $\nu(\mathbf{x})$ and porosity $n^*(\mathbf{x})$. We consider the problem of hydraulically boundary constrained one-dimensional flows induced by hydraulic pulse tests conducted on a heterogeneous porous medium where the spatial variations in these four parameters follow log-normal distributions such that the effective values for the permeability, the elastic modulus, Poisson’s ratio and porosity are given by \tilde{K} , \tilde{E} , $\tilde{\nu}$ and \tilde{n}^* .

The partial differential equation governing the potential field $\Phi(\mathbf{x}, t)$ associated with transient flow in the porous medium is given by (6) with the parameters assigned their respective effective values: i.e.

$$\left(\frac{\tilde{K}}{\mu(\tilde{n}^*C_w + \tilde{C}_{sk})} \right) \nabla^2 \Phi(\mathbf{x}, t) = \frac{\partial \Phi(\mathbf{x}, t)}{\partial t} \tag{25}$$

where \tilde{C}_{sk} is the compressibility of the porous skeleton given by

$$\tilde{C}_{sk} = \frac{3(1 - 2\tilde{\nu})}{\tilde{E}} \tag{26}$$

We first consider the problem of a hydraulic pulse testing conducted in a semi-infinite fluid saturated one-dimensional region. The boundary ($z=0$) is in contact with a fluid reservoir of volume V_w . The partial differential equation governing the problem is given by

$$\left(\frac{\tilde{K}}{\mu(\tilde{n}^*C_w + \tilde{C}_{sk})} \right) \frac{\partial^2 \Phi}{\partial z^2} = \frac{\partial \Phi}{\partial t}; \quad z \in (0, \infty); \quad t > 0 \tag{27}$$

subject to the boundary and regularity conditions

$$\Phi_a \left(\frac{\partial \Phi}{\partial z} \right)_{z=0} = \left(\frac{\partial \Phi}{\partial t} \right)_{z=0}; \quad \Phi(\infty, t) \rightarrow 0 \tag{28}$$

and the initial condition

$$\Phi(z, 0) = 0 \tag{29}$$

In the event the porous medium has an initial potential, the boundary condition (29) should be changed to accommodate the initial condition [53]. In (28), $\Phi_a = (A\tilde{K}/\mu V_w C_w)$, where A is the cross-sectional area of the sample and V_w is the volume of the fluid that is in contact with the surface area A and subjected to a potential of the form

$$\Phi(0, t) = \Phi_0 \delta(t) \quad (30)$$

where $\delta(t)$ is the Dirac delta function. The solution of the initial boundary value problem defined by (27) to (30) can be obtained using Laplace transform techniques and the result of interest to the hydraulic pulse test, namely the time-dependent decay of the fluid potential in the pressurized region, is given by

$$\frac{\Phi(t)}{\Phi_0} = \exp(\Omega^2 t) \operatorname{Erfc}\left(\sqrt{\Omega^2 t}\right) \quad (31)$$

where $\operatorname{Erfc}(x)$ is the complementary error function defined by

$$\operatorname{Erfc}(x) = \frac{2}{\sqrt{\pi}} \int_0^\infty \exp(-\zeta^2) d\zeta \quad (32)$$

and

$$\Omega^2 = \left(\frac{A^2 \tilde{K} (\tilde{n} C_w + \tilde{C}_{sk})}{\mu V_w^2 C_w^2} \right) \quad (33)$$

The result (31) can be used to examine the accuracy of the representation of the properties $K(\mathbf{x})$, $E(\mathbf{x})$, $\nu(\mathbf{x})$ and $n(\mathbf{x})$ through their corresponding effective representations \tilde{K} , \tilde{E} , $\tilde{\nu}$ and \tilde{n}^* .

7. Computational modelling of transient flow

In this section, we examine the transient flow problem described previously within the context of its application to a typical heterogeneous porous medium. Hydraulic pulse tests are usually conducted on geomaterials of relatively low permeability. For consistency of application, however, and for the purposes of illustration of the general approach, we shall consider the decay of a hydraulic pulse conducted on a material such as Indiana Limestone, with the identical range of permeabilities derived from the steady-state tests described previously. In order to examine the effects of heterogeneity on the performance of the pulse test, we construct an idealized heterogeneous porous medium where the upper and lower bounds for the variables are specified and variation in the properties relevant to the examination of hydraulic pulse tests (i.e. the permeability $K(\mathbf{x})$, the elastic modulus $E(\mathbf{x})$, the Poisson's ratio $\nu(\mathbf{x})$ and the porosity $n^*(\mathbf{x})$) are all assumed to correspond to log-normal distributions. The theoretical result for the one-dimensional hydraulic pulse test assumes that the domain in which the pulse test is carried out is semi-infinite. In the computational simulations, however, the one-dimensional domain modelled is finite. In a computational simulation, the size of the one-dimensional domain needs to be increased so that the regularity condition in (28) is satisfied. There is no absolute value that can be chosen to model the domain, since for such a diffusive-type problem this will depend on

the permeability of the porous medium. Computations were performed by progressively increasing the length of the one-dimensional domain until the response of the hydraulic pulse test is un-influenced by the far-field boundary condition. This procedure is referred to as the domain selection process and becomes important in correctly modelling, computationally, the transient effects in hydraulic pulse tests [52–56]. In the domain selected for computational modelling, each sub-region is assigned a property corresponding to a value that is randomly selected from the log-normal distribution. To preserve plausibility of the variations in the distributions representing a porous medium, it is assumed that the compressibility of the porous skeleton and the porosity correlate directly with the permeability. Results of experimental investigations reported in the literature (see e.g. [24,57–59]) indicate that the elastic modulus, Poisson’s ratio and porosity of the Indiana Limestone can vary in the ranges of:

$E \in (23.3, 70.0)$ GPa; $\nu \in (0.207, 0.300)$; $n^* \in (0.16, 0.30)$, respectively. Using these ranges in conjunction with (26), we can determine the range of the porous skeleton compressibility, which becomes

$$C_{sk} \in (0.1714 \times 10^{-7} ; 0.7562 \times 10^{-7}) \text{ m}^2 / \text{kN} \tag{34}$$

The computations commence by using a cuboidal element of the heterogeneous porous medium similar to that used in Figure 3 in order to model the steady state behaviour. The effective permeability of the heterogeneous porous medium corresponding to the log-normal variation, with extreme values identified previously, can be determined using the procedures identical to those presented in Sections 3 and 4. In order to determine the effective compressibility of the cuboidal element with heterogeneous porouskeletal compressibility, we computationally model a cuboidal region that is subjected separately to states of oedometric compression and pure shear [60,61], which give estimates for

$$\tilde{E}_{oed} = \frac{\tilde{E}(1 - \tilde{\nu})}{(1 + \tilde{\nu})(1 - 2\tilde{\nu})}; \quad \tilde{G} = \frac{\tilde{E}}{2(1 + \tilde{\nu})} \tag{35}$$

and these results yield $\tilde{E} = 32.06$ GPa and $\tilde{\nu} = 0.216$, which can be used to estimate the effective compressibility \tilde{C}_{sk} of the heterogeneous porous skeleton defined by (26). Ideally, the estimation of the effective properties of the heterogeneous porous skeleton should be performed by subjecting the entire heterogeneous element, separately, to oedometric compression in three orthogonal directions and pure shear in three orthogonal planes. An alternative approach is to directly subject the porous medium with elastic heterogeneity to isotropic compression and to compute the effective compressibility of the medium by determining the overall volume change. Both these procedures give almost the same estimate for \tilde{C}_{sk} of $\sim 0.53 \times 10^{-7} \text{ m}^2/\text{kN}$. Finally, the effective porosity of the cuboidal porous element with heterogeneity in the porosity can be calculated in a straightforward manner using the arithmetic mean. Avoiding details, it can be shown that the effective values of the parameters of interest for analytically modelling the response of the hydraulic pulse tests are as follows:

$$\tilde{K} = 73.96 \times 10^{-15} \text{ m}^2; \quad \tilde{C}_{sk} = 0.53 \times 10^{-10} \text{ m}^2/\text{N}; \quad \tilde{n}^* = 0.196 \tag{36}$$

The averaging technique for the estimation of \tilde{n}^* involves the summation of the void fraction V_v^* of all the 1000 elements in the synthetic porous region where the porosity also conforms to a log-normal distribution, which ranges between $n^* \in (0.16, 0.30)$. The average porosity is defined by $\tilde{n}^* = V_v^*/V$, where V is the volume of the synthetic porous domain. Attention is now focused on modelling the hydraulic pulse test where the entire domain of interest is modelled by finite elements and with properties assigned spatial variations that conform to log-normal distributions, taking into consideration the correlations indicated previously. We consider the problem of a hydraulic pulse test conducted on a 508 mm cuboidal region. The exterior lateral boundaries of the region are subjected to null Neumann boundary conditions for fluid flow. No other boundary conditions can be prescribed on the deformations since the governing partial differential equation strictly relates to the potential field $\Phi(z, t)$. In order to simulate the fluid reservoir of volume V_w that is subjected to the pressure pulse defined by (30), we consider a finite enclosure with cross-sectional area A that is in contact with the porous medium and in which the boundaries are non-deformable and the permeability of the region is five orders of magnitude larger than a plausible value for the rock that is being tested. At the start of the hydraulic pulse tests, the fluid pressure in the reservoir region will be finite, whereas the fluid pressure in the porous domain will be zero. This discontinuity in the fluid pressures is accommodated for in the analytical solution of the hydraulic pulse test, whereas numerical instabilities can be encountered in the computational simulations if suitable mesh refinement and time discretizations are not adopted. Ideally, to account for this requirement, the computational treatment should consider adaptive algorithms in space and time. In this study, however, extensive mesh refinement and small time steps are adopted to ensure unconditional stability of the solutions. The mesh refinement used in the study is illustrated in Figure 9. Both the “fluid” and the porous domains are discretized using Lagrangian (C_0 continuity) tetrahedral elements. The computational approach is used to develop a solution to the problem of a one-dimensional hydraulic pulse test that is conducted on a heterogeneous porous medium where the relevant parameters exhibit log-normal variations. The computational solutions were developed using the multi-physics code COMSOL™. In addition to the parameters defined by (32), we note that

$$\begin{aligned} A &= 0.2581 \text{ m}^2; & V_w &= 0.1311 \text{ m}^3 \\ C_w &= 4.541 \times 10^{-7} \text{ m}^2/\text{kN}; & \mu &= 10^{-3} \text{ N s m}^{-2} \end{aligned} \quad (37)$$

From (36) and (37), we have

$$\Omega^2 = 0.197 \text{ s}^{-1} \quad (38)$$

Figure 10 illustrates the fluid pressure decay in the pressurized cavity as determined from the *four* approaches:

- (1) The computational solution for the pulse test conducted in a completely heterogeneous domain with log-normal spatial variations in the *permeability*, the *elastic modulus*, *Poisson's ratio* and *porosity* over specified ranges as obtained from actual experimental data on Indiana Limestone used in the permeability tests.

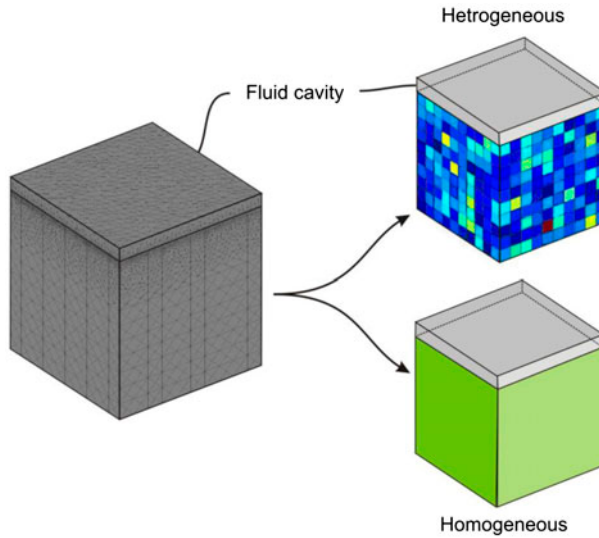


Figure 9. (colour online) Finite-element mesh for one-dimensional pulse tests (consisting of 127,583 tetrahedral elements).

- (2) The computational results for the pressure decay in the pressurized cavity as determined from a computational solution of the one-dimensional pulse test that uses the effective properties for the permeability determined through the geometric mean estimate, the effective compressibility determined by subjecting the entire cuboidal region to oedometric compression and pure shear, that allows estimation of the effective compressibility of the heterogeneous elastic medium using (35), and the effective porosity determined by an averaging procedure and for which the effective values are summarized in (36).
- (3) The analytical result for the pressure-pulse decay conducted in a region of infinite length as defined by (31) and calculated using the data given by (36).

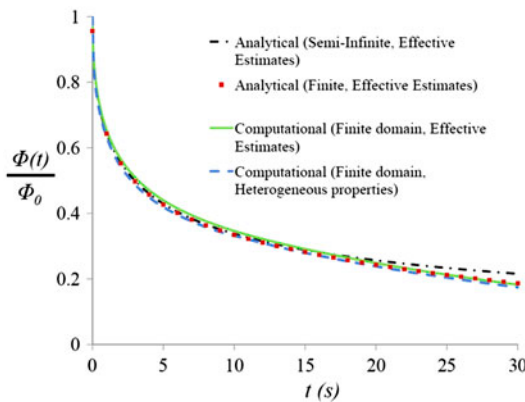


Figure 10. (colour online) Results of one-dimensional pulse tests – Simulations involving Indiana Limestone.

- (4) The analytical result for the pressure pulse test conducted in a region of *finite length* as given by Hsieh et al. [62] using effective estimates of the parameters involved.

A comparison between the four estimates (Figure 10) clearly indicates that the estimate for the *effective permeability* based on the concept of the *geometric mean* is able to accurately duplicate fluid transients in the hydraulic pulse tests. It must be emphasized that for consistency in the presentation, the computations for the hydraulic pulse tests were performed for the block of Indiana Limestone where the permeability is usually determined from steady-state techniques rather than pulse techniques. As such the pulse decay is very rapid. The computations can be performed for ultra-low permeability materials such as the Lindsay-Cobourg Limestone [56] with permeability in the range from 10^{-22} m² to 10^{-21} m² or Stanstead Granite [57] with permeability in the range from 10^{-20} m² to 10^{-19} m², which gives rise to relatively lengthy pulse decay periods.

8. Conclusions

The results of this research indicate that spatial distributions of isotropic permeability can be accommodated through the introduction of the measure of an *effective permeability* and that the *geometric mean* is a reliable estimate for the *effective permeability*. For the geometric mean concept to be applicable, the hydraulic heterogeneity of the porous medium should not include dominant features of hydraulic conductivity that represent a high degree of anisotropy and/or evidence of fractures. Also, for the *geometric mean*-based representation of the effective hydraulic conductivity to be applicable, Darcy's law should be satisfied and the distribution of hydraulic heterogeneity should be a *log-normal distribution*. The validity of the assertion is established through experiments conducted on Indiana Limestone and through computational simulations applicable to cuboidal, annular and toroidal porous domains, which utilize the experimental data. The analysis is also extended to the study of hydraulic pulse tests that are conducted on fluid-saturated porous media where the permeability, the elastic modulus, Poisson's ratio and the porosity all vary spatially in a log-normal manner. The results indicate that the pulse decay observed in the heterogeneous porous medium corresponds quite closely to the decay curves estimated using effective estimates. It could be concluded that when a hydraulic pulse test is conducted in a heterogeneous porous medium, the value of the permeability determined from the pulse test is more likely to represent the *geometric mean* of the permeability.

Acknowledgements

The work described in this paper was supported in part through the *Max Planck Research Prize in the Engineering Sciences* awarded by the Max Planck Gesellschaft, Berlin, Germany and in part through *NSERC Discovery Grant*, both awarded to A.P.S. Selvadurai and through the *NSERC PGS-D scholarship* awarded to P.A. Selvadurai. The authors are grateful to a referee for the detailed comments that led to improvements in the presentation of subject matter.

References

- [1] J. Bear, C.F. Tsang and G. de Marsily, *Flow and Contaminant Transport in Fractured Rock*, Academic Press, San Diego, CA, 1993.
- [2] A.P.S. Selvadurai, *Water Resour. Res.* 39 (2003) p.1204, WRR 001742.
- [3] A.P.S. Selvadurai, *Int. J. Num. Analyt. Meth. Geomech.* 28 (2004) p.191.
- [4] N.A. Chapman and I.G. McKinley, *The Geological Disposal of Nuclear Waste*, Wiley, New York, NY, 1987.
- [5] A.P.S. Selvadurai and T.S. Nguyen, *Engineering Geology* 47 (1996) p.379.
- [6] E.E. Alonso and J. Alcoverro, *Int. J. Rock Mech. Mining Sci.* 42 (2005) p.611.
- [7] A.P.S. Selvadurai, *Geophys. Res. Lett.* 33 (2006) p.L08408.
- [8] J.D. Byerlee and W.F. Brace, *Bull. Seism. Soc. Am.* 62 (1972) p.657.
- [9] A. Nur and J.R. Booker, *Science* 175 (1972) p.885.
- [10] J.R. Rice, *J. Geophys. Res.* 111(B05) (2006) p.311.
- [11] M.H. Dickson and M. Fanelli, eds., *Geothermal Energy*, John Wiley, New York, NY, 1995.
- [12] W.A. Duffield and J.H. Sass, *Geothermal Energy-Clean Power from the Earth's Heat*, Technical Report C1249, U.S. Geological Survey, Reston, VA, 2003.
- [13] S. Bachu and J.J. Adams, *Energy Conver. Manage.* 44 (2003) p.3151.
- [14] C.-F. Tsang, J.T. Birkholzer and J. Rutqvist, *Environ. Geol.* 54 (2008) p.1723.
- [15] A.P.S. Selvadurai, *Geophys. Res. Lett.* 36(14) (2009) p.1029.
- [16] A.P.S. Selvadurai, in *Geomechanics of CO₂ Storage Facilities*, Ch. 5, G. Pijaudier-Cabot and J.-M. Pereira, eds., John Wiley & Sons, Hoboken, 2013, pp. 75–94.
- [17] A. Henriette, C.G. Jacquin and P.M. Adler, *Physico-Chem. Hydrodyn.* 11(1989) p.63.
- [18] J.H. Cushman, ed., *Dynamics of Fluids in Hierarchical Porous Media*, Academic Press, London, 1990.
- [19] P.M. Adler, *Porous Media: Geometry and Transports*, Butterworth-Heinemann, London, 1992.
- [20] L.W. Gelhar, *Stochastic Subsurface Hydrology*, Prentice Hall, Upper Saddle River, NJ, 1993.
- [21] U. Hornung, ed., *Homogenization in Porous Media*, Springer-Verlag, Berlin, 1997.
- [22] C. Tegnander and T. Gimse, *Math. Geol.* 30 (1998) p.717.
- [23] K. Markov and L. Preziosi, eds., *Heterogeneous Media-micromechanics Modeling Methods and Simulations*, Birkhauser-Verlag, Boston, MA, 2000.
- [24] A.P.S. Selvadurai and P.A. Selvadurai, *Proc. Roy. Soc., Math. Phys. Sci. A* 466 (2010) p.2819.
- [25] A.P. Suvorov and A.P.S. Selvadurai, *Comp. Geotech.* 38 (2011) p.721.
- [26] A.P.S. Selvadurai, *Int. J. Num. Analytical Meth. Geomech.* 35 (2010) p.639.
- [27] P. Kitanidis, *Introduction to Geostatistics*, Cambridge University Press, Cambridge, 1997.
- [28] D. Hristopulos and G. Christakos, *Phys. Rev. E* 55 (1997) p.7288.
- [29] J.B. Keller, *Trans. Porous Med.* 43 (2001) p.395.
- [30] D. Zhang, *Stochastic Methods for Flow in Porous Media, Coping with Uncertainties*, Academic Press, San Diego, CA, 2002.
- [31] H. Okabe and M.J. Blunt, *M.J. Phys. Rev.* 70 (2004) p.066135.
- [32] P.L. Churcher, P.R. French, J.C. Shaw and L.L. Schramm, *Soc. Pet. Engrs.* (1991). Publ. SPE 21044.
- [33] ILLI, *Indiana Limestone Handbook*, 22nd ed., Indiana Limestone Institute of America, Bedford, IN, 2007.
- [34] A. Głowacki, *The Permeability Hysteresis of Indiana Limestone during Isotropic Compression*, M. Eng. thesis, McGill University, 2006.
- [35] P. Mattar, *Permeability of Intact and Fractured Indiana Limestone*, M. Eng. thesis, McGill University, 2009.

- [36] P.A. Selvadurai, *Permeability of Indiana Limestone: Experiments and Theoretical Concepts for Interpretation of Results*, M. Eng. thesis, McGill University, 2010.
- [37] Y. Ji, P. Baud, V. Vajdova and T.F. Wong, *Oil Gas Sci. Tech.* 67 (2012) p.753.
- [38] O. Wiener, *Abh. Math.-Phys. Kl Königl. Sächs. Ges* 32 (1912) p.509.
- [39] L.D. Landau and E.M. Lifshitz, *Electrodynamics of Continuous Media*, Pergamon Press, Oxford, 1960.
- [40] G. Matheron, *Eléments pour une Théorie des Milieux Poreux*, Masson, Paris, 1967.
- [41] P.R. King and J. Phys, *J. Phys: Math. Gen.* 20 (1987) p.3935.
- [42] A.G. Journel, C.V. Deutsch and A.J. Desbrats, *Power averaging for block effective permeability*, Tech. Rep., Society of Petroleum Engineers, Dallas, 1986.
- [43] G. Dagan, *Trans. Porous Med.* 12 (1993) p.279.
- [44] A.P.S. Selvadurai and B.M. Singh, *Int. J. Solids Struct.* 20 (1984) p.129.
- [45] A.P.S. Selvadurai and B.M. Singh, *Quart. J. Mech. Appl. Math.* 38 (1985) p.233.
- [46] D.J. Goggin, R.L. Thrasher and L.W. Lake, *In Situ* 12 (1988) p.79.
- [47] D.M. Tartakovsky, J.D. Moulton and V. Zlotnik, *Water Resour. Res.* 36(9) (2000) p.2433.
- [48] F.J. Massey Jr, *J. Am. Stat. Assoc.* 46 (1951) p.68.
- [49] C.W. Fetter, *Applied Hydrogeology*, Merrill Publishers, New York, NY, 2001.
- [50] A.P.S. Selvadurai, *Partial Differential Equations in Mechanics, Vol. 1. Fundamentals, Laplace's Equation, Diffusion Equation, Wave Equation*, Springer-Verlag, Berlin, 2000.
- [51] A.P.S. Selvadurai, *Comp. Geotech.* 29 (2002) p.525.
- [52] Earth's Dynamic Systems, Ch.13, earths.info.pdfs/EDS_13.PDF.
- [53] A.P.S. Selvadurai, *Geophys J. Int.* 177 (2009) p.1357.
- [54] A.P.S. Selvadurai and P. Carnaffan, *Can. J. Civil Eng.* 24 (1997) p.489.
- [55] A.P.S. Selvadurai, M.J. Boulon and T.S. Nguyen, *Pure Appl. Geophys.* 162 (2005) p.373.
- [56] A.P.S. Selvadurai, A. Letendre and B. Hekimi, *Environ. Earth Sci.* 64 (2011) p.2047.
- [57] A.P.S. Selvadurai and M. Najari, *Adv. Water Resour.* 53 (2013) p.139.
- [58] M. Najari and A.P.S. Selvadurai, *Env. Earth Sci.* (2013). doi:[10.1007/s12665-013-2945-3](https://doi.org/10.1007/s12665-013-2945-3).
- [59] A.P.S. Selvadurai and A. Głowacki, *Ground Water* 46 (2008) p.113.
- [60] R.O. Davis and A.P.S. Selvadurai, *Elasticity and Geomechanics*, Cambridge University Press, Cambridge, 1996.
- [61] A.P.S. Selvadurai, *Partial Differential Equations in Mechanics, Vol. 2. Fundamentals, The Biharmonic Equation, Poisson's Equation*, Springer-Verlag, Berlin, 2000.
- [62] P.A. Hsieh, J.V. Tracy, C.E. Neuzil, J.D. Bredehoeft and S.E. Silliman, *Int. J. Rock Mech. Min Sci. Geomech. Abstr.* 18 (1981) p.245.